

Optimal control of anisotropic Allen-Cahn equations

Luise Blank¹, Johannes Meisinger¹

Abstract. This paper aims at solving an optimal control problem governed by an anisotropic Allen-Cahn equation numerically. Therefore we first prove the Fréchet differentiability of an in time discretized parabolic control problem under certain assumptions on the involved quasilinearity and formulate the first order necessary conditions. As a next step, since the anisotropies are in general not smooth enough, the convergence behavior of the optimal controls are studied for a sequence of (smooth) approximations of the former quasilinear term. In addition the simultaneous limit in the approximation and the time step size is considered. For a class covering a large variety of anisotropies we introduce a certain regularization and show the previously formulated requirements. Finally, a trust region Newton solver is applied to various anisotropies and configurations, and numerical evidence for mesh independent behavior and convergence with respect to regularization is presented.

Key words. Allen-Cahn equation, anisotropy, quasilinear parabolic equation, optimal control, regularization, discretization, optimality conditions

AMS subject classification. 35K59, 49K20, 49M41, 65M60

1 Introduction

The goal of this paper is to study the optimal control of anisotropic phase field models describing interface evolution. These models are successfully applied e.g. for anisotropic solidification processes like crystal growth (see also [13] and references therein). The defining equations are given by a gradient flow of a Ginzburg-Landau energy. Here several ansatzes exist to incorporate anisotropy. In the pioneering paper [18] the author considers convex anisotropies in order to obtain a well-posed problem. In [14, 20, 21, 23, 27] various approaches are taken to enlarge this also to non-convex anisotropies by adding regularization terms or changing the structure of the energy functional. We pursue to define the Ginzburg-Landau functional resembling [18], i.e.

$$\mathcal{E}(y) := \int_{\Omega} \varepsilon A(\nabla y) + \varepsilon^{-1} \psi(y) \, dx, \quad (1)$$

¹Department of Mathematics, University of Regensburg, D-93040 Regensburg, Germany (luise.blank@ur.de, johannes.meisinger@ur.de)

but using a different class of anisotropy functions $A : \mathbb{R}^d \rightarrow \mathbb{R}$ where $A(p) = \frac{1}{2}|\gamma(p)|^2$ with a so-called density function $\gamma : \mathbb{R}^d \rightarrow \mathbb{R}_{\geq 0}$ (see e.g. [15]). The first part of the functional represents the surface energy while the potential ψ drives the order parameter y to the pure phases given by the local minimizers ± 1 . The interface thickness is proportional to the variable $\varepsilon > 0$. The scaled L^2 -gradient flow of (1) yields the anisotropic Allen-Cahn equation which defines the state equation for our control problem. This reads as

$$\min J(y, u) := \frac{1}{2} \|y(T) - y_\Omega\|_{L^2(\Omega)}^2 + \frac{\lambda}{2\varepsilon} \|u\|_{L^2(Q)}^2 \quad (2)$$

subject to the quasilinear parabolic state equation with potentially nonsmooth A'

$$\begin{aligned} \int_Q \varepsilon \partial_t y \eta + \varepsilon A'(\nabla y)^T \nabla \eta + \frac{1}{\varepsilon} \psi'(y) \eta &= \int_Q u \eta \quad \forall \eta \in L^2(0, T; H^1(\Omega)) \\ y(0) &= y_0 \quad \text{in } \Omega \end{aligned} \quad (3)$$

where $\Omega \subset \mathbb{R}^d$ is a bounded Lipschitz domain, $Q := [0, T] \times \Omega$ denotes the space-time cylinder, $\Sigma := [0, T] \times \partial\Omega$ its boundary and the target function $y_\Omega \in L^2(\Omega)$ as well as the initial state $y_0 \in H^1(\Omega)$ are given. The weak formulation implies the boundary condition $A'(\nabla y)^T \nu = 0$ on Σ where ν is the outer normal. Furthermore note that the weight of the control cost is divided by ε since from practical observations one expects contributions only in vicinity of the interface.

In this paper we focus on the control problem discretized in time and aim at differentiability of the reduced cost functional such that efficient control solvers can be applied. Regarding differentiability considerations and first order conditions we point also to [8, 9, 10] where the authors consider quasilinear elliptic problems related to ours as well as to [25, 26] for a problem with similar time discretization that is also regularized. For eqs. (2) to (3) the time discretization is given as in our paper [6] where existence of optimal controls and the convergence with respect to the time discretization is shown. For convenience we shortly repeat the dG(0) discretization here. Let $I_j := (t_{j-1}, t_j]$ and

$$\begin{aligned} Y_\tau &:= \{y_\tau : Q \rightarrow \mathbb{R} \mid y_\tau(t, \cdot) \in H^1(\Omega), y_\tau(\cdot, x) \text{ constant in } I_j \text{ for } j = 1, \dots, N\}, \\ U_\tau &:= \{u_\tau : Q \rightarrow \mathbb{R} \mid u_\tau(t, \cdot) \in L^2(\Omega), u_\tau(\cdot, x) \text{ constant in } I_j \text{ for } j = 1, \dots, N\}, \end{aligned} \quad (4)$$

and for each interval we label the constant by a subscript, e.g. $y_j := y_\tau|_{I_j}$. The time discretized control problem is then given by

$$\min_{Y_\tau \times U_\tau} J(y_\tau, u_\tau) = \frac{1}{2} \|y_N - y_\Omega\|^2 + \frac{\lambda}{2\varepsilon} \sum_{j=1}^N \tau_j \|u_j\|^2 \quad (5)$$

subject to

$$\begin{aligned} \frac{\varepsilon}{\tau_j} (y_j, \varphi) + \varepsilon (A'(\nabla y_j), \nabla \varphi) + \frac{1}{\varepsilon} (\psi'(y_j), \varphi) &= (u_j, \varphi) + \frac{\varepsilon}{\tau_j} (y_{j-1}, \varphi) \quad \forall \varphi \in H^1(\Omega), \\ & j = 1, \dots, N \end{aligned} \quad (6)$$

where $y_0 \in H^1(\Omega)$ is the given initial value.

Usually the density function γ in $A(p) = \frac{1}{2}|\gamma(p)|^2$ is assumed to be a positive 1-homogeneous function in $C^2(\mathbb{R}^d \setminus \{0\}) \cap C(\mathbb{R}^d)$ (see, e.g., [4, 13, 15, 16]) providing absolutely 2-homogeneity of A . Consequently A'' is absolutely 0-homogeneous and therefore it does not exist at the origin unless γ is an energy norm. Hence the control-to-state operator may not be differentiable. Since numerical methods for nonsmooth optimal control problems are still in its infancy this is problematic for efficient solvers. For a nonsmooth quasilinear elliptic control problem a semismooth Newton method is applied to a relaxed optimality system in [7]. To the best of our knowledge globally convergent methods for parabolic equations without extra regularity requirements do not exist. To circumvent this problem, the present approach is to consider a regularized A by modifying the function γ . We give the details later, when we have introduced the specific form of A which was first proposed in [3, 4]. Furthermore, while for the numerical experiments we use the smooth double-well potential $\psi(y) = \frac{1}{4}(y^2 - 1)^2$, the analysis holds for more general ψ . This is also the case for A . The functions A and ψ shall fulfill at least the assumptions from [6] listed below under a) to guarantee the existence of the optimal control and the existence and convergence of the time discretized optimization problem. The assumptions are further restricted to obtain differentiability of the reduced cost functional. These conditions are met by the regularized A as can be seen in section 4.

Assumptions 1.1.

- a. Assume $A \in C^1(\mathbb{R}^d)$ with A' being strongly monotone and fulfilling the growth condition $|A'(p)| \leq C|p|$.
Let $\psi \in C^1(\mathbb{R})$ be bounded from below and such that it can be approximated by f_n satisfying $f_n \in C^2(\mathbb{R})$, $f_n \rightarrow \psi$ in C^1_{loc} , $-c \leq f_n \leq c(\psi + 1)$, $f_n'' \geq -C_\psi$, $|f_n''| \leq C_n$, with $c, C_\psi, C_n \geq 0$ and $\psi(y_0) \in L^1(\Omega)$ for the given initial data $y_0 \in H^1(\Omega)$.
Furthermore for the time discretization the restriction $\max_j \tau_j < \varepsilon^2/C_\psi$ on the time steps $\tau_j := t_j - t_{j-1}$ holds.
- b. Assume in addition $A \in C^2(\mathbb{R}^d)$ with bounded A'' and let $\psi \in C^2(\mathbb{R})$ where the Nemytskii operator given by ψ'' is continuous from $H^1(\Omega)$ to $L^q(\Omega)$ for some $q > \max\{d/2, 1\}$.

Let us mention that one can find $p > 2$ with $H^1(\Omega) \hookrightarrow L^p(\Omega)$ and $\frac{1}{q} + \frac{2}{p} < 1$, e.g., when $d \in \{1, 2\}$ choose some $p \in (\frac{2q}{q-1}, \infty)$ and for $d \geq 3$ choose $p = \frac{2d}{d-2}$. Such a p will be used in the following. Note that the assumptions imply that A'' is uniformly positive definite and $\psi'' \geq -C_\psi$ holds. Furthermore, the double-well potential fulfills the condition if $d \leq 3$ since ψ'' induces a continuous Nemytskii operator from $L^{2q}(\Omega)$ to $L^q(\Omega)$ (see, e.g., [30, Proposition 26.6]) and the imbedding $H^1(\Omega) \hookrightarrow L^{2q}(\Omega)$ is only valid for $d \leq 3$.

The outline of this paper is as follows. In section 2 we study under above assumptions the Fréchet differentiability of the reduced cost functional for eqs. (5) to (6). As a first step we analyze the differentiability of the state equation in one time step. Then, due to the

implicit discretization one can successively prove differentiability of the control-to-state operator and of the reduced cost functional. The corresponding time discrete adjoint equation is deduced rigorously. Subsequently, in section 3 we give sufficient conditions on the regularization A_δ of A such that the corresponding states converge to the solution of the originally given state equation. Furthermore, also the convergence of a subsequence of global minimizers u_τ^δ with respect to the regularization parameter δ and the time discretization coarseness τ is addressed. While these results hold under above assumptions on A , in the subsequent section we study the class of anisotropies given in [3, 5]. We introduce a regularization for this class by adjusting γ . Furthermore we show that A fulfills Assumptions 1.1.a, and that in addition 1.1.b as well as the conditions in section 3 hold for the regularizations. In the final section we first set up formally the linearized equations needed for a trust region Newton solver applied to the only in time discretized control problem. We provide numerical evidence for convergence with respect to the regularization and for iteration numbers independent of the discretization level. Finally numerical results for various facets of the anisotropy and different configurations are presented.

2 Fréchet differentiability of the reduced cost functional for the time-discretized problem

In this section we investigate the Fréchet differentiability of the cost functional $j_\tau(u_\tau) := J(y_\tau(u_\tau), u_\tau)$ for the time discretized optimal control problem reduced to the control u_τ when the Assumptions 1.1 hold. Hence the first order optimality system can be shown rigorously. Furthermore its derivative is needed for the numerical optimization solver.

As a first step the Fréchet differentiability of the discrete control-to-state operator $S_\tau : U_\tau \rightarrow Y_\tau$ of eq. (6) is shown. Here, the idea is to prove it for a single time step and then to apply the chain rule. Let us recall, that the solution operator $S_\tau : U_\tau \rightarrow Y_\tau$ of eq. (6) is given by mapping u_τ , correspondingly (u_1, \dots, u_N) , to $y_\tau = S_\tau(u_\tau)$ determined by (y_1, \dots, y_N) with

$$y_j = S(\frac{1}{\varepsilon}u_j + \frac{1}{\tau_j}y_{j-1}) \quad \forall j = 1, \dots, N. \quad (7)$$

Here $S : L^2(\Omega) \rightarrow H^1(\Omega), g \mapsto \mathbf{y}$ is defined as the solution operator of the quasilinear elliptic problem

$$(A'(\nabla \mathbf{y}), \nabla \varphi) + (\zeta(\mathbf{y}), \varphi) = (g, \varphi) \quad \forall \varphi \in H^1(\Omega) \quad (8)$$

with

$$\zeta(s) := \frac{1}{\varepsilon^2} \psi'(s) + \frac{1}{\tau_j} s. \quad (9)$$

Note under Assumptions 1.1.a the left-hand side defines a strongly monotone operator. In [6] we have shown the unique existence of the solution. Let us mention that with the restriction on the space dimension $d \leq 3$ a result from [11] for quasilinear elliptic

equations with controls on the Neumann boundary provides solutions in $L^\infty(\Omega)$ if in addition $A'(0) = 0$. Here the restriction on d is due to the use of Stampacchia's method.

The next auxiliary lemma is obtained by subtracting the defining equations, testing with $\mathbf{y} - \tilde{\mathbf{y}}$ and using strong monotonicity of A' and ζ .

Lemma 2.1. *Let Assumptions 1.1.a hold. Then the solution operator S for eq. (8) is Lipschitz continuous with a constant independent of τ for small enough τ , i.e. to be more precise for $g, \tilde{g} \in L^2(\Omega)$ and $\mathbf{y} = S(g)$, $\tilde{\mathbf{y}} = S(\tilde{g})$ it holds*

$$\|\mathbf{y} - \tilde{\mathbf{y}}\|_{H^1(\Omega)} \leq C \|g - \tilde{g}\|_{H^1(\Omega)}. \quad (10)$$

Let us mention that for $y_\tau = S_\tau(u_\tau)$ and $\tilde{y}_\tau = S_\tau(\tilde{u}_\tau)$ it holds also (see [6, Theorem 2.4])

$$\|y_\tau - \tilde{y}_\tau\|_{L^\infty(0,T;L^2(\Omega))} + \|\nabla y_\tau - \nabla \tilde{y}_\tau\|_{L^2(0,T;L^2(\Omega))} \leq C_{A,\psi,T} \|u_\tau - \tilde{u}_\tau\|_{L^2(0,T;H^1(\Omega))}. \quad (11)$$

Due to difficulties related to a required norm-gap for the differentiability of the A' -term, the implicit function theorem is not applicable directly (cf. [24]). Since it is more illuminating, we follow the approach in [10, 8, 11] to show Gâteaux differentiability. We have to add some work afterwards in order to upgrade to Fréchet differentiability.

Theorem 2.2. *Let Assumptions 1.1 hold. Then the solution operator $S : L^2(\Omega) \rightarrow H^1(\Omega)$ of eq. (8) is Gâteaux differentiable and the directional derivative $S'(g)v = z$ is given with $\mathbf{y} = S(g)$ by $z \in H^1(\Omega)$ such that*

$$(A''(\nabla \mathbf{y}) \nabla z, \nabla \varphi) + (\zeta'(\mathbf{y})z, \varphi) = (v, \varphi) \quad \forall \varphi \in H^1(\Omega). \quad (12)$$

Furthermore there exists a C independent of $g \in L^2(\Omega)$ and τ with

$$\|z\|_{H^1(\Omega)} \leq C \|v\|_{L^2(\Omega)}. \quad (13)$$

Proof. Due to the Assumptions 1.1 the bilinear form defined by the left-hand side of (12) is elliptic with an ellipticity constant independent of $\mathbf{y} = S(g)$ and is continuous given that $|(\zeta'(\mathbf{y})z, \varphi)| \leq C \|\zeta'(\mathbf{y})\|_{L^q(\Omega)} \|z\|_{L^p(\Omega)} \|\varphi\|_{L^p(\Omega)} \leq C \|\zeta'(\mathbf{y})\|_{L^q(\Omega)} \|z\|_{H^1(\Omega)} \|\varphi\|_{H^1(\Omega)}$. Hence the Lax-Milgram theorem provides existence and uniqueness of the solution of eq. (12) for $v \in L^2(\Omega)$ and—using $\zeta'(s) \geq -\frac{1}{\varepsilon^2} C_\psi + \frac{1}{\tau} \geq c > 0$ for small enough τ —the estimate (13) holds for the solutions independently of g and τ .

For $v \in L^2(\Omega)$ and $\rho > 0$ let us consider

$$(A'(\nabla \mathbf{y}_\rho), \nabla \varphi) + (\zeta(\mathbf{y}_\rho), \varphi) = (g + \rho v, \varphi). \quad (14)$$

Subtracting the equation with $\rho = 0$ and dividing by ρ , we obtain

$$\left(\frac{A'(\nabla \mathbf{y}_\rho) - A'(\nabla \mathbf{y})}{\rho}, \nabla \varphi \right) + \left(\frac{\zeta(\mathbf{y}_\rho) - \zeta(\mathbf{y})}{\rho}, \varphi \right) = (v, \varphi) \quad \forall \varphi \in H^1(\Omega). \quad (15)$$

Lemma 2.1 yields for $z_\rho := \frac{1}{\rho}(\mathbf{y}_\rho - \mathbf{y})$

$$\|z_\rho\|_{H^1(\Omega)} \leq C\|v\|_{L^2(\Omega)} \quad \forall \rho. \quad (16)$$

Therefore there exists a subsequence with $z_{\rho_n} \rightharpoonup z$ in $H^1(\Omega)$. We now show that this solves eq. (12) by taking the limit in eq. (15). This implies that z is in fact the desired Gâteaux derivative. For the first term we have

$$\int_{\Omega} \frac{1}{\rho_n} \left(A'(\nabla \mathbf{y}_{\rho_n}) - A'(\nabla \mathbf{y}) \right) \nabla \varphi \, dx = \int_{\Omega} \nabla z_{\rho_n}^T A''(w_{\rho_n}) \nabla \varphi \, dx \xrightarrow{n \rightarrow \infty} \int_{\Omega} \nabla z^T A''(\nabla \mathbf{y}) \nabla \varphi \, dx, \quad (17)$$

where $w_{\rho_n}(x) = \nabla \mathbf{y}(x) + s(x)(\nabla \mathbf{y}_{\rho_n}(x) - \nabla \mathbf{y}(x))$ with $s(x) \in [0, 1]$ is some intermediate point. Since $\mathbf{y}_\rho \rightarrow \mathbf{y}$ in $H^1(\Omega)$ as $\rho \rightarrow 0$ (see lemma 2.1) it holds $w_{\rho_n} \rightarrow \nabla \mathbf{y}$ in $L^2(\Omega)$. The convergence follows since ∇z_{ρ_n} converges weakly, and $A''(\cdot)\nabla \varphi$ is a continuous Nemytskii operator from $(L^2(\Omega))^d$ to $(L^2(\Omega))^d$ given $A'' : \mathbb{R}^d \rightarrow \mathbb{R}^{d \times d}$ is continuous and bounded. Therefore it holds $A''(w_{\rho_n})\nabla \varphi \rightarrow A''(\nabla \mathbf{y})\nabla \varphi$ in $(L^2(\Omega))^d$. We proceed analogously with the second term with intermediate values s_{ρ_n} between \mathbf{y}_{ρ_n} and \mathbf{y} using that $\zeta' : H^1(\Omega) \rightarrow L^q(\Omega)$ is a continuous operator.

Hence z fulfills eq. (12). Since the limit is given uniquely by the latter equation, the whole sequence $(z_\rho)_{\rho \geq 0}$ converges weakly to z in $H^1(\Omega)$.

It remains to show the strong convergence in $H^1(\Omega)$. Due to the compact imbedding into $L^2(\Omega)$ only the part $\nabla z_\rho \rightarrow \nabla z$ in $L^2(\Omega)^d$ is left. For this we consider the sequence $\{L_\rho^T \nabla z_\rho\}_{\rho > 0}$ where L_ρ is the Cholesky-decomposition of the s.p.d.-matrix $A''(w_\rho)$. From boundedness and uniformly positive definiteness of A'' , we obtain $c \leq \|L_\rho(x)\| \leq C$ with constants independent from ρ and x . Since $A''(w_\rho) \rightarrow A''(\nabla \mathbf{y})$ in $L^2(\Omega)^{d \times d}$, from the resulting almost everywhere convergence and just stated boundedness one can verify by dominated convergence that

$$L_\rho \rightarrow L \text{ and } L_\rho^{-1} \rightarrow L^{-1} \quad \text{in } L^2(\Omega)^{d \times d},$$

where L is the Cholesky-decomposition of $A''(\nabla \mathbf{y})$. Furthermore we have

$$\begin{aligned} \|L_\rho^T \nabla z_\rho\|_{L^2(\Omega)}^2 &= \int_{\Omega} \nabla z_\rho^T A''(w_\rho) \nabla z_\rho \, dx \leq \int_{\Omega} \nabla z_\rho^T A''(w_\rho) \nabla z_\rho \, dx + \underbrace{(\zeta'(s_\rho) z_\rho, z_\rho)}_{>0} \\ &= (v, z_\rho)_{L^2(\Omega)} \leq C\|v\|_{L^2(\Omega)}^2 \end{aligned}$$

using (15) in the intermediate value formulation and (16). So we can extract from the sequence $\{L_\rho^T \nabla z_\rho\}_{\rho > 0}$ a weakly convergent subsequence whose limit is $L^T \nabla z$, due to the strong convergence of L_ρ . Due to the uniqueness of the limit also the whole sequence converges weakly in $L^2(\Omega)^d$. Furthermore, there exists a $p' < p$ with $\frac{1}{q} + \frac{2}{p'} \leq 1$. Hence the compact imbedding $H^1(\Omega) \hookrightarrow L^{p'}(\Omega)$ provides $z_\rho \rightarrow z$ in $L^{p'}(\Omega)$. Then using $s_\rho \rightarrow \mathbf{y}$ in $H^1(\Omega)$ and given $\zeta' : H^1(\Omega) \rightarrow L^q(\Omega)$ is a continuous operator we have

$$\begin{aligned} \|L^T \nabla z\|_{L^2(\Omega)}^2 &\leq \liminf_{\rho \rightarrow 0} \|L_\rho^T \nabla z_\rho\|_{L^2(\Omega)}^2 = \lim_{\rho \rightarrow 0} [(v, z_\rho) - (\zeta'(s_\rho) z_\rho, z_\rho)] \\ &= (v, z) - (\zeta'(\mathbf{y})z, z) = \|L^T \nabla z\|_{L^2(\Omega)}^2 \end{aligned}$$

and with that we can even deduce $L_\rho^T \nabla z_\rho \rightarrow L^T \nabla z$ in $L^2(\Omega)^d$. Furthermore there exists some dominating function $m \in L^2(\Omega)$ with $|L_\rho^T \nabla z_\rho| \leq m$. Finally, from the pointwise relations

$$\nabla z_\rho = (L_\rho^{-T})(L_\rho^T \nabla z_\rho) \rightarrow (L^{-T})(L^T \nabla z) = \nabla z, \quad |\nabla z_\rho| = |L_\rho^{-T} L_\rho^T \nabla z_\rho| \leq C |L_\rho^T \nabla z_\rho| \leq Cm$$

we get by dominated convergence that $\nabla z_\rho \rightarrow \nabla z$ in $L^2(\Omega)$.

Ultimately, the desired continuity of $S'(g) : L^2(\Omega) \rightarrow H^1(\Omega)$ needed for the Gâteaux differentiability is given by (13). \square

The following theorem upgrades the last result to Fréchet differentiability.

Theorem 2.3. *Let Assumptions 1.1 hold. Then the mapping $S : L^2(\Omega) \rightarrow H^1(\Omega)$ is Fréchet differentiable.*

Proof. For $g_n \rightarrow g$ in $L^2(\Omega)$ lemma 2.1 provides $y_n := S(g_n) \rightarrow y := S(g)$ in $H^1(\Omega)$ and given $v \in L^2(\Omega)$ we set $z_n := S'(g_n)v$, $z := S'(g)v$. Subtracting the defining equations for z_n and z , testing with $(z_n - z) \in H^1(\Omega)$ and inserting 0 terms yields

$$\begin{aligned} 0 &= \int_{\Omega} (A''(\nabla y_n) \nabla z_n - A''(\nabla y) \nabla z)^T (\nabla z_n - \nabla z) dx \\ &\quad + \int_{\Omega} \nabla z^T (A''(\nabla y_n) - A''(\nabla y)) (\nabla z_n - \nabla z) dx \\ &\quad + (\zeta'(y_n) z_n - \zeta'(y_n) z, z_n - z) + (\zeta'(y_n) z - \zeta'(y) z, z_n - z) \\ &\geq C \|\nabla z_n - \nabla z\|_{L^2(\Omega)}^2 - \|A''(\nabla y_n) - A''(\nabla y)\| \|\nabla z\|_{L^2(\Omega)} \|\nabla z_n - \nabla z\|_{L^2(\Omega)} \\ &\quad + C \|z_n - z\|_{L^2(\Omega)}^2 - C \|\zeta'(y_n) - \zeta'(y)\|_{L^q(\Omega)} \|z\|_{L^p(\Omega)} \|z_n - z\|_{L^p(\Omega)} \end{aligned}$$

using the ellipticity of $A''(s)$ and $\zeta'(s)$ with constants independent of s . Given the estimate (13) $\|z\|_{H^1(\Omega)}, \|z_n - z\|_{H^1(\Omega)} \leq c \|v\|_{L^2(\Omega)}$ and it follows

$$\|A''(\nabla y_n) - A''(\nabla y)\| + \|\zeta'(y_n) - \zeta'(y)\|_{L^q(\Omega)} \geq C \frac{\|z_n - z\|_{H^1(\Omega)}^2}{\|v\|_{L^2(\Omega)}^2} \quad \forall v \in L^2(\Omega).$$

Since $A''(\cdot)$ is a continuous operator from $(L^2(\Omega))^d \rightarrow (L^2(\Omega))^{d \times d}$ and $\zeta'(\cdot)$ is a continuous operator from $L^p(\Omega) \rightarrow L^q(\Omega)$, $y_n \rightarrow y$ in $H^1(\Omega)$ provides that the left-hand side goes to 0 as $n \rightarrow \infty$. Hence S is Fréchet differentiable. \square

We now consider the solution operator $S_\tau : U_\tau \rightarrow Y_\tau$ of eq. (6). On each time interval I_j we have $y_\tau(u_\tau)|_{I_j} = y_j(u_1, \dots, u_j) = S(\frac{1}{\varepsilon} u_j + \frac{1}{\tau_j} y_{j-1}(u_1, \dots, u_{j-1}))$. Using the previous shown result for S as well as the chain rule we obtain for $j = 1, \dots, N$

$$\begin{aligned} z_j &:= \frac{dy_\tau(u_\tau)|_{I_j}}{du_\tau} v_\tau = S'(\frac{1}{\varepsilon} u_j + \frac{1}{\tau_j} y_{j-1})(\frac{1}{\varepsilon} v_j + \frac{1}{\tau_j} \frac{dy_\tau(u_\tau)|_{I_{j-1}}}{du_\tau} v_\tau) \\ &= S'(\frac{1}{\varepsilon} u_j + \frac{1}{\tau_j} y_{j-1})(\frac{1}{\varepsilon} v_j + \frac{1}{\tau_j} z_{j-1}) \end{aligned} \tag{18}$$

where we used $z_0 := 0$ and by induction we can state the following theorem.

Theorem 2.4. *Let Assumptions 1.1 hold. Then the operator $S_\tau : U_\tau \rightarrow Y_\tau$ is Fréchet differentiable and consequently also the reduced cost functional $j_\tau : U_\tau \rightarrow \mathbb{R}$ with $j_\tau(u_\tau) := J(S_\tau(u_\tau), u_\tau)$ is Fréchet differentiable with $j'_\tau(u_\tau)v_\tau = (y_N - y_\Omega, z_N) + \frac{\lambda}{\varepsilon}(u_\tau, v_\tau)$, where z_N is given by the solution of the following sequence with $z_0 := 0$*

$$(\varepsilon A''(\nabla y_j) \nabla z_j, \nabla \varphi) + (\frac{1}{\varepsilon} \psi''(y_j) z_j + \frac{\varepsilon}{\tau_j} z_j, \varphi) = (v_j + \frac{\varepsilon}{\tau_j} z_{j-1}, \varphi) \quad \forall j = 1, \dots, N, \quad \varphi \in H^1(\Omega). \quad (19)$$

We note that the z_j satisfy a linearized state equation given by $z_\tau = S'_\tau(y_\tau)v_\tau \in Y_\tau$. Furthermore, eq. (19) is the dG(0) discretization (as used for the state equation) of the in time continuous, linearized state equation

$$\begin{aligned} \varepsilon(\partial_t z, \eta) + \varepsilon(A''(\nabla y) \nabla z, \nabla \eta) + \frac{1}{\varepsilon}(\psi''(y)z, \eta) &= (v, \eta) \quad \forall \eta \in L^2(0, T; H^1(\Omega)) \\ z(0) &= 0 \quad \text{in } \Omega. \end{aligned} \quad (20)$$

Given Assumptions 1.1 the unique solvability of eq. (20) is guaranteed by standard results on parabolic equations.

Let us mention that, while for the forward problem it may be more efficient to use the semi-implicit scheme of [5] where $A'(\nabla y_i)$ is approximated by $M(\nabla y_{j-1})\nabla y_j$, to show Fréchet differentiability with the above technique of applying the solution operator S recursively, higher regularity properties are required. In particular, to our best knowledge, the gradient of the previous time step solution has to be bounded in $L^\infty(\Omega)$ as it appears in the ellipticity coefficient [28].

Let us now define for given y the adjoint equation in the time continuous setting:

$$\begin{aligned} -\varepsilon(\eta, \partial_t p) + \varepsilon(A''(\nabla y) \nabla \eta, \nabla p) + \frac{1}{\varepsilon}(\psi''(y)\eta, p) &= 0 \quad \forall \eta \in L^2(0, T; H^1(\Omega)) \\ p(T) &= y(T) - y_\Omega \quad \text{in } \Omega. \end{aligned} \quad (21)$$

After the substitution $t \mapsto -t$ as for the linearized equation eq. (20) the existence of a unique adjoint p as a solution of eq. (21) follows. In analogy to the discretization of the state equation, but taking into account the backward-in-time nature, we use the piecewise constant time discrete $p_\tau \in P_\tau$, where

$$P_\tau := \{p_\tau : Q \rightarrow \mathbb{R} \mid p_\tau(t, \cdot) \in H^1(\Omega), p_\tau(\cdot, x) \text{ constant in } \hat{I}_j \text{ for } j = 1, \dots, N\}$$

with $\hat{I}_j := [t_{j-1}, t_j)$ and use the notation $p_{N+1} := p(T)$. The Galerkin scheme

$$(\varepsilon A''(\nabla y_j) \nabla \varphi, \nabla p_j) + (\frac{1}{\varepsilon} \psi''(y_j) \varphi + \frac{\varepsilon}{\tau_j} \varphi, p_j) = \frac{\varepsilon}{\tau_j} (\varphi, p_{j+1}) \quad \text{for } j = N, \dots, 1 \quad (22)$$

starting with $p_{N+1} = y_N - y_\Omega$ then determines the approximation p_τ of p . Given (12) and the symmetry of $S'(g_j)$ with $g_j = \frac{1}{\varepsilon} u_j + \frac{1}{\tau_j} y_{j-1}$ and $y_j = S(g_j)$ we have

$$p_j = \frac{1}{\tau_j} S'(g_j) p_{j+1} \quad \text{for } j = N, \dots, 1.$$

With (18) this leads to

$$(z_j, p_{j+1}) = (S'(g_j)(\frac{1}{\varepsilon}v_j + \frac{1}{\tau_j}z_{j-1}), p_{j+1}) = \frac{\tau_j}{\varepsilon}(v_j, p_j) + (z_{j-1}, p_j) \quad (23)$$

for $j = N, \dots, 1$ and consequently we have

$$(y_N - y_\Omega, z_N) = (p_{N+1}, z_N) = \frac{1}{\varepsilon} \sum_{j=1}^N \tau_j (p_j, v_j) = \frac{1}{\varepsilon} (p_\tau, v_\tau).$$

Altogether, we have shown

Corollary 2.5. *Under Assumptions 1.1 the reduced cost functional $j_\tau : U_\tau \rightarrow \mathbb{R}$ is Fréchet differentiable and the derivative can be represented as*

$$\nabla j_\tau(u_\tau) = \frac{1}{\varepsilon}(\lambda u_\tau + p_\tau)$$

where p_τ is the solution of the discrete adjoint equation eq. (22).

3 Convergence with respect to a regularization of A

In the previous section A had to fulfill Assumptions 1.1.a and b. However, as mentioned in the beginning, anisotropy functions A typically fulfill only Assumptions 1.1.a. In order to guarantee Fréchet differentiability for the numerical approach we regularize such an A to A_δ so that in addition Assumptions 1.1.b hold. An example of regularization is given and discussed in eq. (38).

In this section we consider the dependence on δ of the solutions of the in time discretized optimization problem eq. (5). To consider convergence with $\delta \rightarrow 0$ we need that $A'_\delta \rightarrow A'$. However, the results of this section do not require Fréchet differentiability yet, such that Assumptions 1.1.a on A_δ are sufficient. We denote by $y_\tau \in Y_\tau$ the solution of eq. (6) with A , while $y_\tau^\delta \in Y_\tau$ shall be given as the solution of the regularized equation

$$\varepsilon \frac{(y_j^\delta, \varphi) - (y_{j-1}^\delta, \varphi)}{\tau_j} + \varepsilon (A'_\delta(\nabla y_j^\delta), \nabla \varphi) + \frac{1}{\varepsilon} (\psi'(y_j^\delta), \varphi) = (u_j, \varphi) \quad j = 1, \dots, N \quad (24)$$

and $y_\tau^\delta(0, \cdot) = y_0$. As before we define the reduced cost functional by

$$j_{\tau,\delta}(u_\tau) = \frac{1}{2} \|y_N^\delta(u_\tau) - y_\Omega\|_{L^2(\Omega)}^2 + \frac{\lambda}{2\varepsilon} \|u_\tau\|_{L^2(Q)}^2. \quad (25)$$

We note that to not overload the notation, j_δ is used in place of $j_{\tau,\delta}$ as long as it is clear from the context that τ is considered fixed. The goal of this section is to derive a convergence result for minimizers of a sequence of $j_{\tau,\delta}$ to minimizers of $j_{\tau,0}$ in the limit $\delta \rightarrow 0$ and to minimizers of j when additionally $\tau \rightarrow 0$ holds. Therefore some convergence behavior of the δ -dependent solution y_τ^δ is needed that then is combined with results concerning $\tau \rightarrow 0$ from [6]. This will be covered by the following two auxiliary results.

Theorem 3.1. *Let the Assumptions 1.1.a hold and in addition let A'_δ be strongly monotone with a constant C_A independent of δ and let $|A'_\delta(p) - A'(p)| \leq \eta(\delta)$ for all $p \in \mathbb{R}^d$. Then, for fixed y_0 and u_τ and $\max_j \tau_j$ the solutions $y_\tau(u_\tau)$ and $y_\tau^\delta(u_\tau)$ of eq. (6) and eq. (24), respectively, satisfy the following estimate*

$$\|y_\tau(u_\tau) - y_\tau^\delta(u_\tau)\|_{L^\infty(0,T;L^2(\Omega))} + \|\nabla y_\tau(u_\tau) - \nabla y_\tau^\delta(u_\tau)\|_{L^2(0,T;L^2(\Omega))} \leq C_{A,\psi,T}\eta(\delta). \quad (26)$$

Proof. We note down the differences by a prescript Δ , e.g. $\Delta y_\tau := y_\tau - y_\tau^\delta$. With $\frac{1}{2}(a^2 - b^2) \leq (a - b)a$, testing the defining equations eq. (6) and eq. (24) with Δy_j and using that A'_δ is strongly monotone as well as $(\psi'(x) - \psi'(y), x - y) \geq -C_\psi|x - y|^2$, we obtain

$$\begin{aligned} & \frac{1}{2} \left(\|\Delta y_j\|^2 - \|\Delta y_{j-1}\|^2 \right) + \tau_j C_A \|\nabla \Delta y_j\|^2 \\ & \leq (\Delta y_j - \Delta y_{j-1}, \Delta y_j) + \tau_j \left(A'_\delta(\nabla y_j) - A'_\delta(\nabla y_j^\delta), \nabla \Delta y_j \right) \\ & \leq (\Delta y_j - \Delta y_{j-1}, \Delta y_j) + \tau_j \left(A'(\nabla y_j) - A'_\delta(\nabla y_j^\delta), \nabla \Delta y_j \right) + \tau_j \left(A'_\delta(\nabla y_j) - A'(\nabla y_j), \nabla \Delta y_j \right) \\ & = -\frac{\tau_j}{\varepsilon^2} \left(\psi'(y_j) - \psi'(y_j^\delta), \Delta y_j \right) + \tau_j \underbrace{\left(A'_\delta(\nabla y_j) - A'(\nabla y_j), \nabla \Delta y_j \right)}_{\leq \|A'_\delta(\nabla y_j) - A'(\nabla y_j)\| \|\nabla \Delta y_j\| \leq |\Omega| \eta(\delta) \|\nabla \Delta y_j\|} \\ & \leq \frac{\tau_j}{\varepsilon^2} C_\psi \|\Delta y_j\|^2 + \frac{\tau_j C_A}{2} \|\nabla \Delta y_j\|^2 + \frac{|\Omega|^2 \tau_j}{2C_A} \eta(\delta)^2. \end{aligned}$$

In the last step we used scaled Young's inequality with the scaling C_A . We now sum over $j = 1, \dots, J$ and get

$$\frac{1}{2} \|\Delta y_J\|^2 + \frac{C_A}{2} \sum_{j=1}^J \tau_j \|\nabla \Delta y_j\|^2 \leq \frac{1}{2} \frac{|\Omega|^2}{C_A} \eta(\delta)^2 \sum_{j=1}^J \tau_j + \frac{1}{2} \tilde{C}_\psi \sum_{j=1}^J \tau_j \|\Delta y_j\|^2 \quad (27)$$

for all $1 \leq J \leq N_\tau$. Here we defined $\tilde{C}_\psi := \frac{C_\psi}{\varepsilon^2}$. Omitting the gradient term on the left, absorbing the J -th term from the right and using $\frac{1}{(1 - \tilde{C}_\psi \tau_J)} \leq c$, we obtain

$$\|\Delta y_J\|^2 \leq \frac{c|\Omega|^2}{C_A} T \eta(\delta)^2 + c \tilde{C}_\psi \sum_{j=1}^{J-1} \tau_j \|\Delta y_j\|^2.$$

To this we apply the discrete Gronwall Lemma which yields

$$\|\Delta y_J\|^2 \leq \frac{c|\Omega|^2}{C_A} T \eta(\delta)^2 \exp \left(c \tilde{C}_\psi T \right). \quad (28)$$

Inserting this into eq. (27) we finally get for all $J = 1, \dots, N_\tau$

$$C_A \sum_{j=1}^J \tau_j \|\nabla \Delta y_j\|^2 \leq \frac{|\Omega|^2}{C_A} T \eta(\delta)^2 \left(1 + c \tilde{C}_\psi T \exp \left(c \tilde{C}_\psi T \right) \right) \quad (29)$$

which together with eq. (28) yields the inequality eq. (26). \square

We note that here the constant $C_{A,\psi,T}$ depends exponentially on the interface thickness ε as can be seen in eq. (29). When studying the dependence on ε —which is not subject of this paper—a more careful analysis in terms of ε possibly not based on the Gronwall Lemma is necessary.

Combining the estimate (26) with results in [6] we obtain:

Corollary 3.2. *Let the assumptions of theorem 3.1 be fulfilled and $u_\tau, \tilde{u}_\tau \in U_\tau$ be given. Then the estimate*

$$\|y_\tau(u_\tau) - y_\tau^\delta(\tilde{u}_\tau)\|_{L^\infty(0,T;L^2(\Omega))} + \|\nabla y_\tau(u_\tau) - \nabla y_\tau^\delta(\tilde{u}_\tau)\|_{L^2(0,T;L^2(\Omega))} \leq C_{A,\psi,T}(\eta(\delta) + \|u_\tau - \tilde{u}_\tau\|_{L^2(0,T;H^1(\Omega)')) \quad (30)$$

holds. Hence, given a sequence $(u_\tau)_\tau$ with $u_\tau \rightharpoonup u$ in $L^2(0,T;L^2(\Omega))$ for $\tau \rightarrow 0$, there exists $\sigma(\tau)$ with $\lim_{\tau \rightarrow 0} \sigma(\tau) = 0$ such that

$$\max_{t \in [0,T]} \|y(u)|_t - y_\tau^\delta(u_\tau)|_t\|_{L^2(\Omega)} \leq C(\eta(\delta) + \sigma(\tau)). \quad (31)$$

Proof. Estimate eq. (30) follows by zero completion with $y_\tau(\tilde{u}_\tau)$, triangle inequality and estimating the resulting terms by theorem 3.1 and [6, Theorem 2.4], respectively eq. (11). For the second estimate we recall from [6, Theorem 2.6] that if $u_\tau \rightharpoonup u$ in $L^2(0,T;L^2(\Omega))$ there exists $\sigma(\tau)$ with $\lim_{\tau \rightarrow 0} \sigma(\tau) = 0$ such that $\max_{t \in [0,T]} \|y(u)|_t - y_\tau(u_\tau)|_t\|_{L^2(\Omega)} \leq C\sigma(\tau)$. By inserting $y_\tau(u_\tau)$ and using the triangle inequality together with the first estimate one obtains eq. (31). \square

Finally, we finish this section with the following convergence result of global minimizers.

Theorem 3.3. *Let the assumptions of theorem 3.1 be fulfilled and $\lim_{\delta \rightarrow 0} \eta(\delta) = 0$. Denote by u_τ^δ a global minimizer of $j_{\tau,\delta}$. Then it holds:*

1. *Considering $\delta \rightarrow 0$ for fixed $\tau > 0$, there exists a subsequence such that it holds $u_\tau^\delta \rightarrow \underline{u}_\tau$ in U_τ , $y_\tau^\delta(u_\tau^\delta) \rightarrow y_\tau(\underline{u}_\tau)$ in Y_τ and $j_{\tau,\delta}(u_\tau^\delta) \rightarrow j_\tau(\underline{u}_\tau)$ for $\delta \rightarrow 0$. Furthermore \underline{u}_τ is a global minimizer of j_τ .*
2. *Considering $\tau, \delta \rightarrow 0$, there exists a subsequence such that it holds $u_\tau^\delta \rightarrow \underline{u}$ in $L^2(0,T;L^2(\Omega))$, $y_\tau^\delta(u_\tau^\delta) \rightarrow y(\underline{u})$ in $L^2(0,T;L^2(\Omega))$ and $j_{\tau,\delta}(u_\tau^\delta) \rightarrow j(\underline{u})$. Furthermore \underline{u} is a global minimizer of j .*

Proof. 1. Take $\bar{u}_\tau \in U_\tau$ fixed. From theorem 3.1 we obtain $y_\tau^\delta(\bar{u}_\tau) \rightarrow y_\tau(\bar{u}_\tau)$ in Y_τ for $\delta \rightarrow 0$ and therefore from the boundedness of this sequence we obtain

$$\frac{\lambda}{2\varepsilon} \|u_\tau^\delta\|_{L^2(Q)}^2 \leq j_{\tau,\delta}(u_\tau^\delta) \leq j_{\tau,\delta}(\bar{u}_\tau) \leq C.$$

Hence $u_\tau^\delta \rightharpoonup \underline{u}_\tau \in U_\tau$ for a subsequence, which is considered in the following, and consequently $y_N^\delta(u_\tau^\delta) \rightarrow y_N(\underline{u}_\tau)$ in $L^2(\Omega)$ my, see corollary 3.2. Using the definition of $j_{\tau,\delta}$ in eq. (25) leads to

$$j_\tau(\underline{u}_\tau) \leq \liminf_{\delta \rightarrow 0} j_{\tau,\delta}(u_\tau^\delta) \leq \limsup_{\delta \rightarrow 0} j_{\tau,\delta}(u_\tau^\delta) \leq \lim_{\delta \rightarrow 0} j_{\tau,\delta}(u_\tau) = j_\tau(u_\tau) \quad \forall u_\tau \in U_\tau. \quad (32)$$

Hence \underline{u}_τ is a minimizer. Since we can also choose \underline{u}_τ on the righter part of eq. (32), in addition we obtain $j_{\tau,\delta}(u_\tau^\delta) \rightarrow j_\tau(\underline{u}_\tau)$.

Since we already have $u_\tau^\delta \rightharpoonup \underline{u}_\tau$, to obtain the strong convergence $u_\tau^\delta \rightarrow \underline{u}_\tau$ in U_τ it remains to check that the norms converge. This follows from

$$\frac{\lambda}{2\varepsilon} \|u_\tau^\delta\|_{L^2(Q)}^2 = j_{\tau,\delta}(u_\tau^\delta) - \frac{1}{2} \|y_N^\delta(u_\tau^\delta) - y_\Omega\|_{L^2(\Omega)}^2 \rightarrow j_\tau(\underline{u}_\tau) - \frac{1}{2} \|y_N(\underline{u}_\tau) - y_\Omega\|_{L^2(\Omega)}^2 = \frac{\lambda}{2\varepsilon} \|\underline{u}_\tau\|_{L^2(Q)}^2.$$

2. First we choose an arbitrary but fixed $\bar{u} \in L^2(0, T; L^2(\Omega))$ and a sequence $\bar{u}_\tau \in U_\tau$ with $\lim_{\tau \rightarrow 0} \bar{u}_\tau = \bar{u}$ in $L^2(0, T; L^2(\Omega))$. Hence $\lim_{\delta, \tau \rightarrow 0} y_\tau^\delta(\bar{u}_\tau)|_T = y(\bar{u})|_T$ in $L^2(\Omega)$ due to eq. (31). As above it holds

$$\frac{\lambda}{2\varepsilon} \|u_\tau^\delta\|_{L^2(Q)}^2 \leq \frac{1}{2} \|y_\tau^\delta(\bar{u}_\tau)|_T - y_\Omega\|_{L^2(\Omega)}^2 + \frac{\lambda}{2\varepsilon} \|\bar{u}_\tau\|_{L^2(Q)}^2 \leq C.$$

Hence we can deduce a subsequence denoted in the same way with $u_\tau^\delta \rightharpoonup u$ in $L^2(0, T; L^2(\Omega))$. Then corollary 3.2 yields that $y_\tau^\delta(u_\tau^\delta)|_T \rightarrow y(u)|_T$ in $L^2(\Omega)$ and hence $j(u) \leq \liminf_{\tau, \delta \rightarrow 0} j_{\tau,\delta}(u_\tau^\delta)$. Respectively, given some arbitrary $\tilde{u} \in L^2(0, T; L^2(\Omega))$ and a sequence \tilde{u}_τ with $\tilde{u}_\tau \rightarrow \tilde{u}$ we obtain $\lim_{\tau, \delta \rightarrow 0} j_{\tau,\delta}(\tilde{u}_\tau) = j(\tilde{u})$. Then the assertions follows as in (1). \square

4 The regularization of a class of anisotropies

Before we continue with simulations for optimal control of anisotropic phase field models we have to specify the anisotropy function A . As mentioned in the introduction, this function typically is 2-homogeneous. This in general however conflicts with the requirement of A being twice continuously differentiable. Therefore this section's goal is to specify the employed A , to introduce an appropriate regularization A_δ and to show that A satisfies Assumptions 1.1a. and A_δ fulfills in addition Assumptions 1.1b. This guarantees that the results from [6] and the preceding chapters can be applied. First, recall from the introduction that A can be written as

$$A(p) = \frac{1}{2} |\gamma(p)|^2 \quad \forall p \in \mathbb{R}^d, \quad (33)$$

where the so-called density function $\gamma : \mathbb{R}^d \rightarrow \mathbb{R}_{\geq 0}$ with $\gamma \in C^2(\mathbb{R}^d \setminus \{0\}) \cap C(\mathbb{R}^d)$ shall be positive 1-homogeneous. The terminology 'density function' goes back to the study of sharp interface models, where the surface energy of the interface between a solid and liquid phase, say, is given by $|\Gamma|_\gamma = \int_\Gamma \gamma(\nu) ds$. In the isotropic case $\gamma(p) = |p|$ this

would reduce to the area of the interface $|\Gamma|_\gamma = |\Gamma|$. The authors of [1, 15] show for the Allen-Cahn equation eq. (3)—with A defined as in eq. (33)—that in the limit $\varepsilon \rightarrow 0$ the zero level sets converge to a sharp interface Γ moving with $V = \gamma(\nu)\kappa_\gamma$ if $u = 0$. While there exist several approaches to define γ , like e.g. in [18] or in [13], we constrain ourselves to a class of anisotropies for which the density function γ is introduced in [3]. The corresponding phase field ansatz is studied e.g. in [5]. In the following they are referred to as BGN-anisotropies. They allow for the modelling and approximation of a large class of common anisotropies. Also they are well suited to model crystal growth, since crystals build characteristic faces. The basic observation is that for the metric $(\cdot, \cdot)_{\tilde{G}}$ defined by symmetric positive definite \tilde{G} , the surface area element can be expressed as $\gamma(\nu) = \sqrt{\nu^T G \nu}$ with $G = \det(\tilde{G})^{\frac{1}{d-1}} \tilde{G}^{-1}$ (see [4]). This motivates the choice of the class of density functions γ given by

$$\gamma(p) = \sum_{l=1}^L \gamma_l(p), \quad \text{where } \gamma_l(p) = \sqrt{p^T G_l p} \quad (34)$$

and $G_l \in \mathbb{R}^{d \times d}$ are symmetric and positive definite. Note that for $p \neq 0$ the derivative of A can then be computed as

$$A'(p) = \gamma(p)\gamma'(p) = \sum_{l,m} \frac{\gamma_m(p)}{\gamma_l(p)} G_l p \quad (35)$$

and A' is continuous also at $p = 0$ with $A'(0) = 0$.

The second derivative exists for $p \neq 0$ and is given by

$$A''(p) = \gamma(p)\gamma''(p) + \gamma'(p)\gamma'(p)^T, \quad (36)$$

where

$$\gamma''(p) = \sum_l \left(\frac{G_l}{\gamma_l(p)} - \frac{G_l p (G_l p)^T}{\gamma_l(p)^3} \right).$$

We note that $A'' : \mathbb{R}^d \setminus \{0\} \rightarrow \mathbb{R}^{d \times d}$ is continuous and $A''(p)$ is positive definite with constants independent of p . Moreover we have Lipschitz-continuity and strong monotonicity of A' . These properties follow from results in [16] where the authors need in addition to the given properties of γ , namely continuity on \mathbb{R}^d , twice continuously differentiability on $\mathbb{R}^d \setminus \{0\}$, positive homogeneity of degree one, $\gamma(p) > 0$ for $p \neq 0$ and the following relation

$$q^T \gamma''(p) q \geq C |q|^2 \quad \forall p, q \in \mathbb{R}^d \text{ with } p^T q = 0 \text{ and } |p| = 1.$$

The latter can be shown by an application of the Cauchy-Schwarz inequality

$$q^T \gamma''(p) q = \sum_l \left(\frac{q^T G_l q}{\gamma_l(p)} - \frac{(q^T G_l p)^2}{\gamma_l(p)^3} \right) \geq \sum_l \left(\frac{q^T G_l q}{\gamma_l(p)} - \frac{\gamma_l(p)^2 \gamma_l(q)^2}{\gamma_l(p)^3} \right) = 0,$$

where equality does not hold for $p^T q = 0$ and the compactness of the set given by $p^T q = 0$, $\|p\| = \|q\| = 1$.

Our goal for regularizing A is that $A_\delta \in C^2(\mathbb{R}^d)$ shall fulfill the requirements for the existence of an optimal control, that the derivative shall be simple to evaluate and that the influence on the interfacial region (i.e. $\nabla y \not\approx 0$) shall be little. Our approach is to modify the γ_l , but one could also think of regularizing e.g. the quotient appearing in the sum in eq. (35). Among various choices we considered the most promising was to alter the functions γ_l by a small shift of δ , i.e.

$$\gamma_l^\delta := \sqrt{\gamma_l^2 + \delta} \quad (37)$$

where $\delta > 0$. This we use in the following and denote the resulting regularizations by A_δ and γ_δ . Both are now in $C^\infty(\mathbb{R}^d)$. A very convenient property for this choice is that $\gamma_\delta(p) = \tilde{\gamma}((p, \sqrt{\delta})^T)$ where $\tilde{\gamma}$ is defined employing the matrices $\tilde{G}_l := \begin{pmatrix} G_l & \\ & 1 \end{pmatrix}$. Hence one can also view the regularized anisotropy A_δ on \mathbb{R}^d as an unregularized BGN-anisotropy \tilde{A} on \mathbb{R}^{d+1} for which above properties hold.

The derivatives still have the same structures as in eq. (35) and eq. (36) namely

$$A'_\delta(p) = \sum_{l,m} \frac{\gamma_m^\delta(p)}{\gamma_l^\delta(p)} G_l p, \quad (38)$$

$$A''_\delta(p) = \gamma_\delta(p) \gamma''_\delta(p) + \gamma'_\delta(p) \gamma'_\delta(p)^T, \quad (39)$$

$$\text{with } \gamma''_\delta(p) = \sum_l \left(\frac{G_l}{\gamma_l^\delta(p)} - \frac{G_l p (G_l p)^T}{\gamma_l^\delta(p)^3} \right), \quad (40)$$

though these hold in the regularized version for all $p \in \mathbb{R}^d$. Note that for $L = 1$, i.e. for $A(p) = \frac{1}{2} p^T G p$ which includes the isotropic case, it holds $A'_\delta = A'$. This is a particularly convenient property as in this case A is already smooth by itself and hence there is no need for regularization anyway. Due to

$$A'_\delta(p) = \left(\tilde{A}' \left(\frac{p}{\sqrt{\delta}} \right) \right)_{1,\dots,d}, \quad A''_\delta(p) = \left(\tilde{A}'' \left(\frac{p}{\sqrt{\delta}} \right) \right)_{1,\dots,d} \quad (41)$$

for $\delta > 0$ the Lipschitz-continuity and strong monotonicity of \tilde{A}' provide these properties for A'_δ with constants independent of δ . Moreover, since \tilde{A}'' induces uniformly equivalent norms on \mathbb{R}^{d+1} the same holds for A''_δ . Hence $A''_\delta(p)$ is bounded independent of p . Using $A_\delta(0) \geq A(0) = 0$ we obtain $c|p|^2 \leq A_\delta(p)$ with $c > 0$. This inequality holds also for A due to the 2-homogeneity. Moreover, all constants can be chosen independently of δ . The only exception is the upper bound in the growth condition $A_\delta(p) \leq A_\delta(0) + C|p|^2$ due to $A_\delta(0)$. Finally, Hölder-continuity of $A'_\delta(p)$ with respect to δ follows also with the formulation (41) and the Lipschitz continuity of \tilde{A}' . Summarized we can state

Lemma 4.1. *The mappings $A_\delta : \mathbb{R}^d \rightarrow \mathbb{R}$ for $\delta \geq 0$ (with $A_{\delta=0} := A$ as shorthand notation) have the following properties:*

- a) A_δ fulfill the growth condition $c|p|^2 \leq A_\delta(p) \leq C_\delta + C|p|^2$ for all p with positive constants c, C, C_δ , where only C_δ may depend on δ .
- b) A'_δ are Lipschitz-continuous and strongly monotone on \mathbb{R}^d with constants independent of δ and $A'_\delta(0) = 0$.
- c) A''_δ induce uniformly equivalent norms on \mathbb{R}^d for $\delta > 0$, i.e. there exist constants c_0, C such that

$$c_0\|q\|^2 \leq q^T A''_\delta(p)q \leq C\|q\|^2 \quad \forall p, q \in \mathbb{R}^d, \delta > 0$$

and $A''_\delta(0) = L \sum_{l=1}^L G_l$. Furthermore, if $\delta = 0$ the same holds true for all $p \neq 0$.

- d) $A'_{(\cdot)}(p)$ is Hölder-continuous with exponent $1/2$ and with a constant independent of p . Especially it holds

$$|A'_\delta(p) - A'(p)| \leq C\sqrt{\delta} \quad \forall p \in \mathbb{R}^d, \delta > 0. \quad (42)$$

In particular the Assumptions 1.1 are fulfilled if $\delta > 0$, Assumptions 1.1a. hold for A and the convergence assumption with respect to $\delta \rightarrow 0$ in theorem 3.3 hold.

5 Numerical results

In the last part of this paper we report some numerical findings. When we consider fixed delta in this chapter, we drop the corresponding index in the relevant quantities to keep the presentation lucid. We also consistently use the smooth double-well potential $\psi(s) = \frac{1}{4}(1 - s^2)^2$ which defines $C_\psi = 1$. Our numerical approach for solving the regularized optimization problem is to first discretize in time and then apply an optimization algorithm on this semi-discretized problem. The arising equations and first order condition have rigorously been analyzed in the previous chapters. Finally, each step in the algorithm is discretized also in space where we use global continuous, piecewise linear finite element approximations.

Preliminary numerical results have been obtained by a line search method based on the gradient ∇j_τ . However, since we have not seen any relevant differences in the computed controls and states we only present here results using second order informations—which are formally derived in the following—to gain efficiency in the solver. As algorithm to solve for a local minimizer we apply the trust region Newton method [12] to the reduced cost functional $j_\tau : U_\tau \rightarrow \mathbb{R}$. It is a common globalization of Newton's method which is needed due to the non-convexity of the problem. The main idea is to determine at each iterate u_τ an approximate solution $\delta \bar{u}_\tau$ of the quadratic subproblem

$$\min_{\|\delta u_\tau\| \leq \sigma} (\nabla j_\tau(u_\tau), \delta u_\tau) + \frac{1}{2}(\nabla^2 j_\tau(u_\tau)\delta u_\tau, \delta u_\tau), \quad (43)$$

where $\sigma > 0$ parameterizes the size of a trust region in U_τ where this model is considered to be sufficiently valid. The proper choice of σ is controlled by the trust region method. The solution to eq. (43) is determined by the Steihaug-CG method [22], which iteratively applies the CG-steps to the the first order condition of the unconstrained version of the subproblem $\nabla^2 j_\tau(u_\tau) \delta u_\tau = -\nabla j_\tau(u_\tau)$, and additionally handles the cases when a CG-iterate $\delta \tilde{u}_\tau$ exceeds the trust region boundary or j has at u_τ nonpositive curvature in direction δu_τ , i.e. $(\nabla^2 j_\tau(u_\tau) \delta \tilde{u}_\tau, \delta \tilde{u}_\tau) \leq 0$. Finally the new trust region iterate is set to $u_\tau + \delta \tilde{u}_\tau$.

Let us summarize for convenience the formulas of the last sections:

$$j_\tau(u_\tau) = \frac{1}{2} \|y_\tau(T) - y_\Omega\|^2 + \frac{\lambda}{2\varepsilon} \|u_\tau\|^2 \quad (44)$$

$$\nabla j_\tau(u_\tau) = \frac{1}{\varepsilon} (\lambda u_\tau + p_\tau), \quad (45)$$

where $y_\tau = S_\tau(u_\tau)$ is given by the state equation eq. (6) and $p_\tau = (S'_\tau(u_\tau))^*(y_\tau(T) - y_\Omega)$ is given by the time discrete adjoint equation eq. (22).

The derivative of y_τ in direction of δu_τ we denote by δy_τ , i.e. δy_τ solves the linearized state equation eq. (19) with $v = \delta u_\tau$. This derivative is employed to compute the Hessian as can be seen below.

The second derivative required only here for the Newton approach (see subproblem (43)), in particular its action on an L^2 -function, we deduce formally. We obtain

$$\nabla^2 j_\tau(u_\tau) \delta u_\tau = \frac{1}{\varepsilon} (\lambda \delta u_\tau + \delta p_\tau). \quad (46)$$

Here, for the given solution $p_\tau(u_\tau)$ of eq. (22) the derivative

$$\delta p_\tau := \frac{dp_\tau(u_\tau)}{du_\tau} \delta u_\tau$$

fulfills the so called additional adjoint equation. In time discrete form it is given by $\delta p_{N+1} := \delta y_N$ and

$$\begin{aligned} \varepsilon(A''_\delta(\nabla y_j) \nabla \varphi, \nabla \delta p_j) + \left(\frac{1}{\varepsilon} \psi''(y_j) \varphi + \frac{\varepsilon}{\tau_j} \varphi, \delta p_j\right) &= (\varphi, \frac{\varepsilon}{\tau_j} \delta p_{j+1}) \\ - \varepsilon(A'''_\delta(\nabla y_j) [\nabla \varphi, \nabla \delta y_j], \nabla p_j) - \frac{1}{\varepsilon} (\psi'''(y_j) \varphi \delta y_j, p_j) &\quad \text{for } j = 1, \dots, N. \end{aligned} \quad (47)$$

As for eq. (22) the unique existence of the solution is guaranteed. The time-continuous counterpart is given by

$$\begin{aligned} - \varepsilon(\eta, \partial_t \delta p) + \varepsilon(A''_\delta(\nabla y) \nabla \eta, \nabla \delta p) + \frac{1}{\varepsilon} (\psi''(y) \eta, \delta p) &= \\ - \varepsilon(A'''_\delta(\nabla y) [\nabla \eta, \nabla \delta y], \nabla p) - \frac{1}{\varepsilon} (\psi'''(y) \eta \delta y, p) &\quad \forall \eta \in L^2(0, T; H^1(\Omega)) \end{aligned} \quad (48)$$

$$\delta p(T) = \delta y(T) \quad \text{in } \Omega$$

and they are related by the discontinuous Galerkin time discretization as for the adjoint equation. Note that each of the discretized equations has a time continuous counterpart (cf. eqs. (3), (20), (21) and (48)). In fact, eqs. (20), (21) and (48) are the equations you

would expect to get as the adjoint and corresponding linearized equations for eq. (3). Thus at least on a formal level it holds that the approaches *first discretize then optimize* and *first optimize then discretize* commute for the implicit time discretization in the sense of [17, chapters 3.2.2 and 3.2.3]. Also discretization and optimization are interchangeable for the spatial discretization if one chooses the same ansatz spaces for y and p . Consequently, one expects to obtain for the optimization solver iteration numbers independent of the discretization level. This is strengthened by numerical observations in section 5.2. Note that in general the 3-tensor A_δ''' appearing in eq. (48) is not symmetric, so we have to keep care of order in the corresponding term. In the implementation A_δ''' is determined by automatic differentiation—stating an explicit formula does give no new insight. Moreover, since $\nabla y = 0$ in the pure phases one is particularly interested in the behavior of $A_\delta'''(p)$ when $p \rightarrow 0$. However, $\tilde{A}'''(\sqrt{\delta} \binom{p}{1})$ behaves like $1/\sqrt{\delta}$ due to the 2-homogeneity of \tilde{A} (see eq. (41)). Hence $\lim_{p \rightarrow 0} A_\delta'''(p)$ cannot be bounded independently of δ . Numerically we see this problem for values $\delta < 10^{-13}$.

To keep the computational cost moderate we set $d = 2$ in all experiments. Furthermore, throughout this section we use as a spatial domain the square $\Omega = (-1, 1)^2$ and as the time horizon $[0, T]$ with $T = 1.625 \cdot 10^{-2}$, we set the parameters $\varepsilon = \frac{1}{14\pi}$ and $\lambda = 0.01$ and—if not mentioned otherwise—the regularization parameter $\delta = 10^{-7}$. We choose the constant time step size $\tau = 1.625 \cdot 10^{-4}$, which fulfills the condition $\tau \leq \varepsilon^2/C_\psi$ and Ω is uniformly discretized with 129×129 grid points. Moreover by numerical evidence we know that the interface is resolved sufficiently with 6-14 mesh points across the interface. Each computation started with $u^{(0)} \equiv 0$.

We have looked at various set-ups that mainly vary by y_0 , y_Ω and the final time T . For the anisotropies determined by G_l we used three different choices, that are listed in the following.

1. isotropic case: $\gamma(p) = \|p\|_2$ this would belong to the choice

$$G = \begin{pmatrix} 1 & 0 \\ 0 & 1 \end{pmatrix}. \quad (49)$$

Note that in this case regularization is not necessary. In addition, the regularization would cancel out as can be seen in eq. (38) and as it is also discussed in the corresponding text thereunder.

2. regularized l_1 -norm:

$$G_1 = \frac{1}{2} \begin{pmatrix} 1 & 0 \\ 0 & \epsilon \end{pmatrix}, \quad G_2 = \frac{1}{2} \begin{pmatrix} \epsilon & 0 \\ 0 & 1 \end{pmatrix}, \quad (50)$$

with some small parameter ϵ that we set to $\epsilon = 0.01$ (not to be confused with the interface parameter ε). For $\epsilon = 0$ this reduces to $\gamma(p) = \frac{1}{\sqrt{2}} \|p\|_{\ell_1}$.

3. form of a smoothed hexagon:

$$G_l = \frac{1}{3} \begin{pmatrix} \cos(\alpha_l) & -\sin(\alpha_l) \\ \sin(\alpha_l) & \cos(\alpha_l) \end{pmatrix} \begin{pmatrix} 1 & 0 \\ 0 & \epsilon \end{pmatrix} \begin{pmatrix} \cos(\alpha_l) & \sin(\alpha_l) \\ -\sin(\alpha_l) & \cos(\alpha_l) \end{pmatrix}, \quad (51)$$

where $\alpha_l = \frac{\pi}{3}l$, $l = 1, 2, 3$ and ϵ as before.

Note that in contrast to the choices in [4] we divide the matrices by their total number L . By this scaling the costs between the different anisotropies becomes more comparable, since by numerical observation the velocity of the shrinkage is approximately equal. This can also be seen on the Wulff shapes, which are defined as $\mathcal{W} := \{q \in \mathbb{R}^d : \sup_{p \in \mathbb{R}^d \setminus \{0\}} \frac{p^T q}{\gamma(p)} \leq 1\}$, see [29], and which are visualized for above choices of γ in fig. 1. Without the rescaling the Wulff-shape of the hexagon anisotropy would extend approximately to the label 2.0 on each axis.

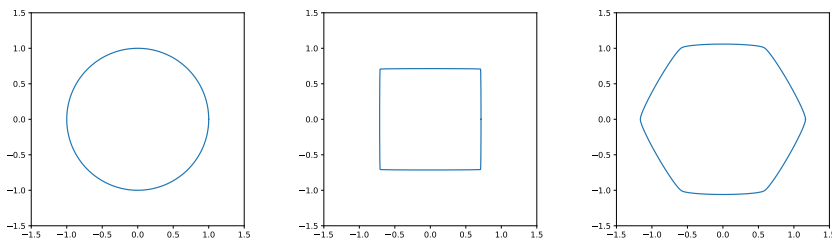


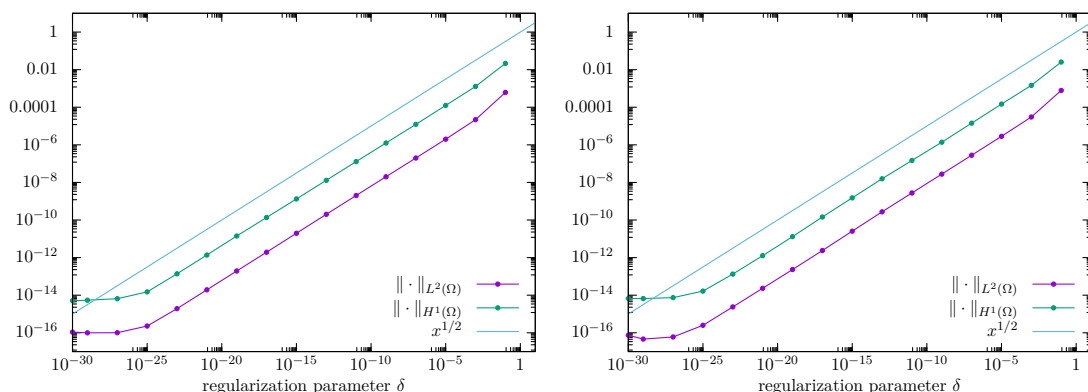
Figure 1: Wulff shapes of isotropic, l_1 - and hexagon-anisotropy.

As computing framework we used FEniCS [2] or rather its C++ interface DOLFIN [19]. The simulations were carried out on an HP EliteDesk 800 G4 workstation containing an Intel Core i7-8700 CPU with 12 cores à 3.20GHz and 16 GB of RAM.

In the following subsections we support the convergence result of theorem 3.1 concerning the regularization, we give numerical evidence for mesh independent behavior in the solution process and we present optimal control results for different anisotropies and different desired states, including star like objects and necessary topology changes.

5.1 Dependence on the regularization parameter δ

First we analyze numerically the dependence of the solution of the state equation on the parameter δ . As a setting we start from a circle of radius 0.5 and look at the evolution of the state only using $u = 0$. A plot containing the results for the choices of both anisotropies respectively is given in Figure 2. We have plotted both the difference of the states in $L^2(\Omega)$ as well as $H^1(\Omega)$ at the end point T . Since errors accumulate during the time evolution the errors at T should be a good metric for comparison. With the additionally plotted function $f(x) = x^{1/2}$ the figure clearly exhibits the convergence order 1/2 which is expected according to eqs. (26) and (42), i.e. it equals the approximation order of A'_δ to A' .



(a) Results for the regularized l_1 -norm.

(b) Results for the hexagon anisotropy.

Figure 2: Comparison of $\|y_\tau^\delta(T) - y_\tau(T)\|$ in the $L^2(\Omega)$ and $H^1(\Omega)$ -norms for different values of δ .

When considering the numerical solution of the optimization problem, according to our experience there is only weak dependence of the number of the trust region as well as of the Steihaug-CG iterations when varying δ . They stay nearly the same as in tables 1 and 2 and are therefore not listed here. If δ is such small that rounding errors accumulate for A_δ'' and even more for A_δ''' (and consequently for the solutions of the respective equations) the algorithm may not converge. However, for $\delta \geq 10^{-10}$ the algorithm was always robust.

5.2 Mesh independent behavior

In this section we numerically investigate the mesh dependence of the problem solver. More concretely we look at the number of trust region iterations, called *TR steps* in the following tables, as well as at the number of Steihaug-CG steps that are needed to solve the quadratic subproblems. Since Steihaug algorithm consists of early stopping criteria given by the trust region algorithm their amount might change drastically during the progress of the algorithm. Therefore we rather look at the average amount of steps, called *mean CG* in the following tables, that are needed to decrease the residuum by 6 orders of magnitude for trust region steps where this kind of measurement is possible. In addition we also take the maximum amount, called *max CG* as an indicator. These numbers of CG iterations reflect on the conditioning of the linear systems corresponding to the quadratic subproblems. As final time we choose in these experiments $T = 2 \times 10^{-3}$. The remaining parameters are left unchanged. We inspect the dependence on the space discretization by fixing $\tau = 10^{-4}$ and varying $h = 2/N$. For analyzing the dependence on the step size τ we fix the spatial mesh size using $N = 128$.

As model problem for the isotropic case, we consider the control of a circle from radius

$r = 0.5$ to $r = 0.55$, where the results can be found in table 1. One cannot observe a clear tendency that would suggest dependency of the maximal or mean number of CG iterations and of the trust region steps on the granularity, as is expected by the discussion in the introduction of this section. Only the amount of total computing time increases with the number of unknowns. Let us mention that in case of $\tau = 10^{-4}$ and $N = 516$ the reduced optimization problem has around 5.4 million unknowns given by the amount of discretization points of u . If $\tau = 10^{-6}$ and $N = 128$ the number of unknowns is roughly 33.3 million. Due to the parallelization of the algorithm and the non-commutativity of floating point operations the results might vary slightly among runs sharing the same configuration.

N	64	128	256	512	τ	10^{-4}	$10^{-4.5}$	10^{-5}	$10^{-5.5}$	10^{-6}
max CG	38	48	38	39	max CG	48	60	34	34	34
mean CG	21.2	22.7	18.8	20.4	mean CG	22.7	22.2	18.4	18.0	18.5
TR steps	12	16	11	12	TR steps	16	11	9	8	8
time (s)	17	72	235	1196	time (s)	72	105	213	706	2032

Table 1: Dependence on N and τ for the isotropic case.

Next we do the same analysis for the anisotropic Allen-Cahn equation with the regularized l_1 -norm. Here we choose y_0 and y_Ω the same, i.e. we try to keep a square constant. The outcomes are listed in table 2. Again, almost no dependence on the discretization parameters is observed. Numbers for the average Steihaug steps as well as for the total trust region steps rather seem to ameliorate for more accurate computations. Finally, we

N	64	128	256	512	τ	10^{-4}	$10^{-4.5}$	10^{-5}	$10^{-5.5}$	10^{-6}
max CG	60	40	40	39	max CG	40	40	39	35	35
mean CG	30.0	22.0	21.3	21.0	mean CG	22.0	21.8	24.0	20.0	20.7
TR steps	10	6	6	6	TR steps	6	6	7	5	5
time (s)	24	66	194	1193	time (s)	66	161	537	1127	3306

Table 2: Dependence on N and τ for the regularized l_1 -norm where $y_\Omega = y_0$.

list in table 3 the results for the control of a circle to a star with four fingers as can be seen in fig. 3. Here more control is necessary and the solution process takes significantly more trust region steps. Also the number of CG iterations are increased compared to table 2. While this indicates the dependency on the control configuration the results concerning the CG-iterations still show a behavior independent of the discretization level. A slight increase in the number of trust region steps is present.

N	64	128	256	512	τ	10^{-4}	$10^{-4.5}$	10^{-5}	$10^{-5.5}$	10^{-6}
max CG	185	207	243	167	max CG	207	180	175	181	175
mean CG	129.0	127.7	139.7	117.0	mean CG	127.7	153.0	148.0	130.5	137.3
TR steps	71	83	106	125	TR steps	83	95	146	126	108
time (s)	95	641	4068	23657	time (s)	641	1462	5476	13753	46297

Table 3: Dependence on N and τ for the simulation circle to 4-star for the regularized l_1 -norm.

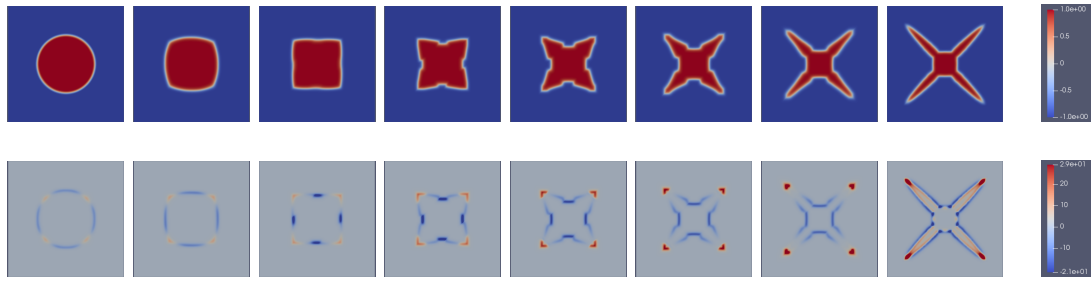
5.3 Numerical examples for different desired states and anisotropies

Finally we present solution for three different objectives: the evolution to star-like structures, the splitting of geometries and the merging of geometries. For the presented figures which show the evolution of the control u we employed a scaling of the color that was adjusted to the values at $t \approx T/2$. Hence this allows to see where in Ω the control is present although its values may be clipped on some images. To see how much the system is controlled at which time, we in addition include figures showing the $L^2(\Omega)$ -norm of the control over time.

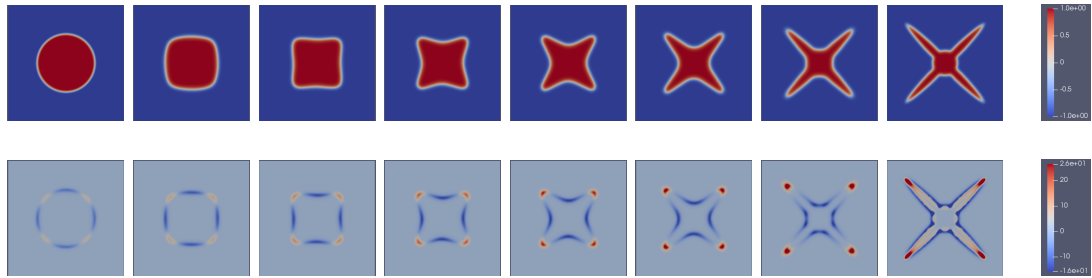
5.3.1 Evolution to star-like structures

In the first experiment we start from a circle of radius 0.5 and try to steer it to a star-like structure with 4 or 6 fingers respectively. The images of the time evolution of the corresponding states and controls can be found in figs. 3 and 4. The state is given by the Allen-Cahn equation with the regularized l_1 -norm anisotropy for the ‘4-star’ target, and with the ‘hexagon’ anisotropy for the ‘6-star’ target. In addition we present the results in both cases for the isotropic evolution equation. In practice the choice of Allen-Cahn equation is given by the model equation and not by the desired state.

Qualitatively the main observation is that in all cases the control takes place in a neighborhood of the interface. Moreover, the evolution is controlled essentially in the second half of the time interval. This can be particularly seen in fig. 5 where the $L^2(\Omega)$ -norms of the control are plotted over the time t . On the t -axis we indicated the times at which the states and controls were sampled for figs. 3 and 4. While for the isotropic case the middle part seems to grow nearly linearly, for the cases of the regularized l_1 -norm and the hexagon anisotropy one observes bigger jumps intersected by approximately constant parts. The first plateau comes from the fact that at the first part the evolution follows the nearly uncontrolled Allen-Cahn flow to get a square-like, respectively a hexagon-like shape. Only then the control truly enters to initiate the development of the fingers with the strongly non-convex parts. From that point onwards more control is needed for the anisotropic cases than for the isotropic case but towards the end they approximately overlap. The last peak arises from the fact that much of the control is spent to form the details of the fingers in the last few time steps.

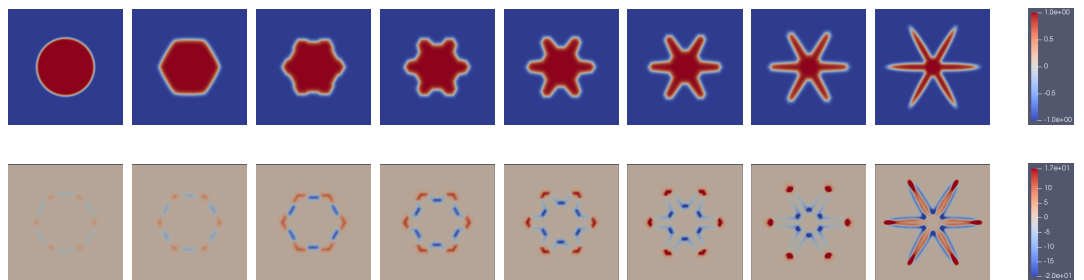


(a) Results for the regularized l_1 -norm.

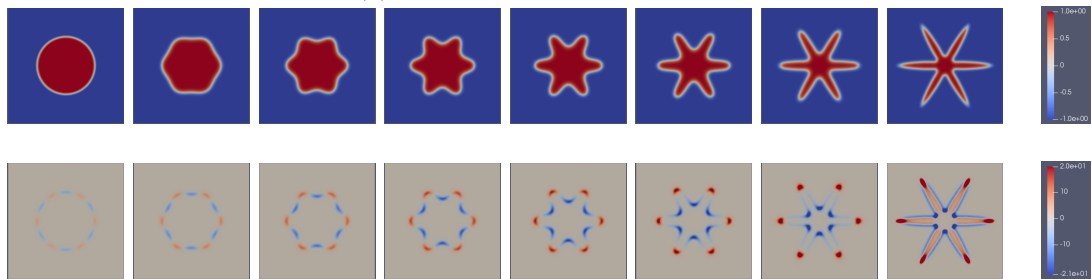


(b) Results for the isotropic case.

Figure 3: ‘circle to 4-star’ solutions: states in the first and third row and controls in the second and fourth row .

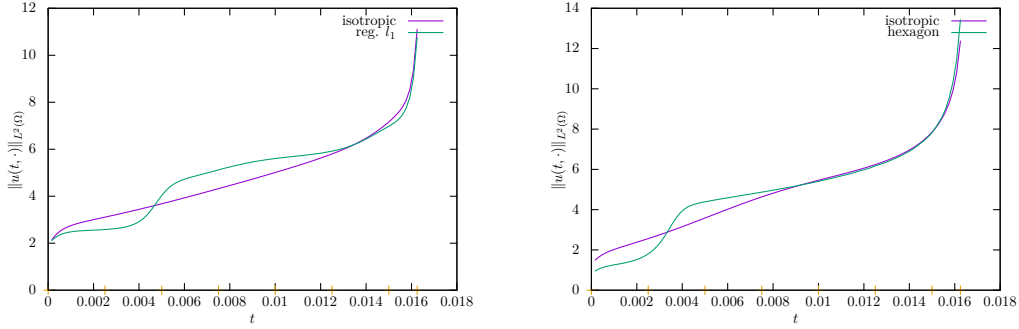


(a) Results for the hexagon case.



(b) Results for the isotropic case.

Figure 4: ‘circle to 6-star’ solutions: states in the first and third row and controls in the second and fourth row.



(a) Results for ‘circle to 4-star’ cf. fig. 3. (b) Results for ‘circle to 6-star’ cf. fig. 4.

Figure 5: Time evolution $\|u(t, \cdot)\|_{L^2(\Omega)}$.

In table 4 the computed (local) minima are listed together with their single constituents—the difference of the optimal state to the desired state $j_1 = \|y - y_\Omega\|_{L^2(\Omega)}^2$ as well as the contribution of the control $j_2 = \frac{\lambda}{2\varepsilon} \|u\|_{L^2(Q)}^2$. We note that the (local) optima for the isotropic case are slightly below their anisotropic counterparts.

	4 star		6 star	
	iso	l_1	iso	hexa
$j(u)$	0.102184	0.107378	0.115034	0.12248
$j_1 + j_2$	0.0115987 + 0.0905854	0.0108916 + 0.0964865	0.0122366 + 0.102798	0.0156595 + 0.106821

Table 4: Values of the cost functional.

5.3.2 Splitting and merging geometries

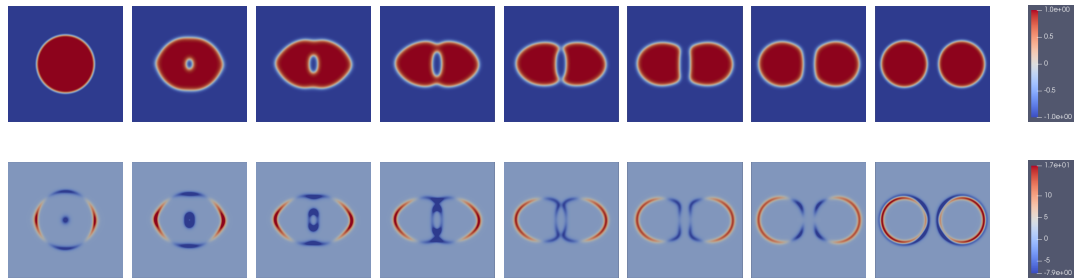
Finally we consider examples where topology changes are necessary to aim at the target. In fig. 6 we present the results for splitting a circle, a square and a hexagon into two of such respectively. The underlying model equation uses the corresponding (an-)isotropy. In fig. 7 the solutions of merging two of these objects into one are given. Here the target objects are the initial states of the splitting examples and vice versa. The norms of the corresponding controls over the time can be seen in fig. 8. To avoid potential confusion, we point out that the scales of the ordinates are adapted to better fit the plots.

While the hexagon is splitted by squeezing it together vertically, the circle is controlled to develop first a hole in the middle and then to increase the hole until the split is present. The square is divided at the whole middle line simultaneously—as far as we could see visually. The controls are largest at times where they force topology changes as can be observed in fig. 8a.

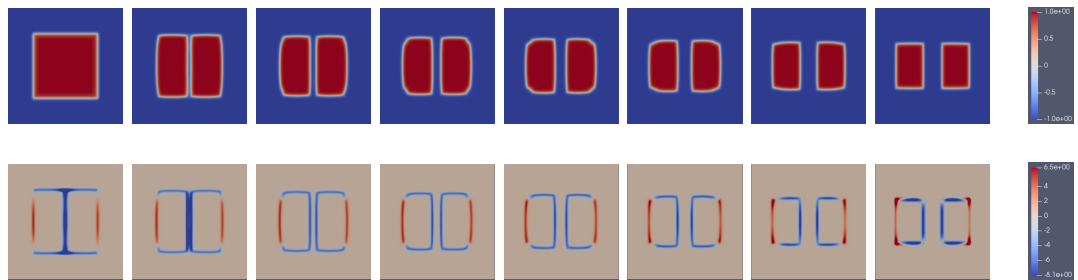
Considering the examples for ‘merging’ (see fig. 7) we observe a very similar behavior of the states as for the ‘splitting’ solutions, but backwards in time. There is less control

necessary which is indicated by the values for j_2 in tables 5 and 6 where the cost functionals are given as for the star like examples before. For the isotropic and hexagon example the splitting cost is higher by a factor of approximately 1.5. That the difference is not bigger is probably due to the short time interval that forces the evolution of the gradient flow to be accelerated to obtain the target in time—a phenomenon present for splitting as well as for merging, with comparable impact. This also leads to the nearly constant time behavior for a long period—as can be seen in fig. 8b.

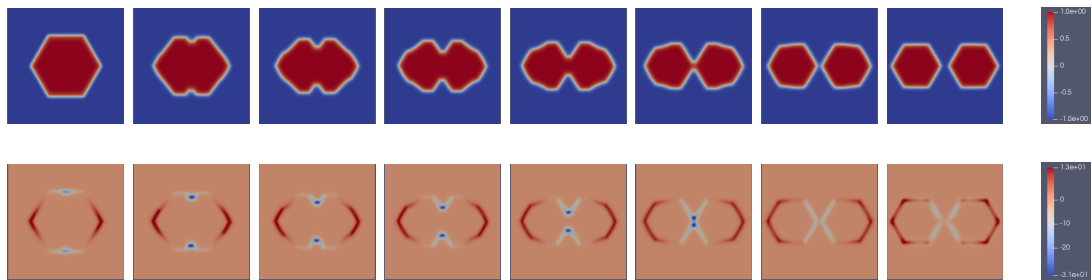
Altogether these examples have demonstrated that it is possible to steer to a variety of shapes even if they have a different topology as the initial state. Also targeting strong crystal-like structures is possible which might find use in material science or chemical applications.



(a) Result for the ‘splitting circle’ in the isotropic case.

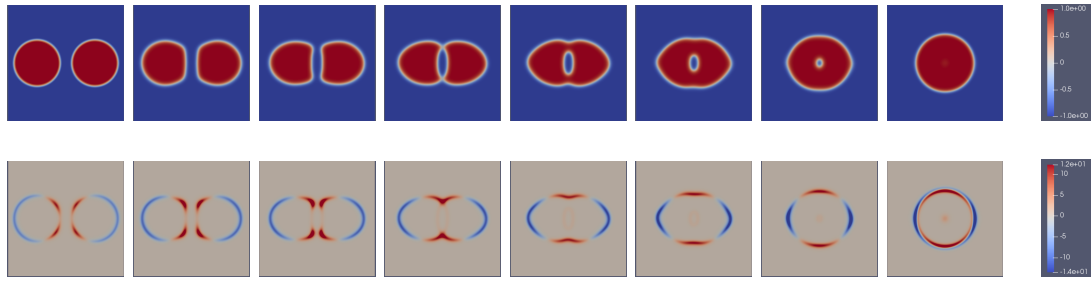


(b) Result for the ‘splitting square’ with the regularized l_1 -norm.

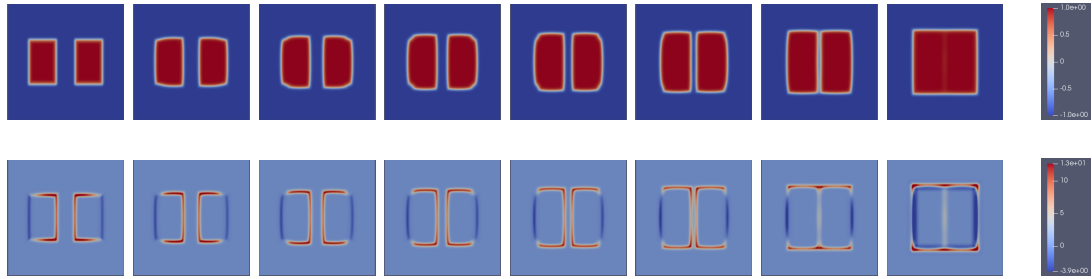


(c) Result for the ‘splitting hexagon’ using the hexagon anisotropy.

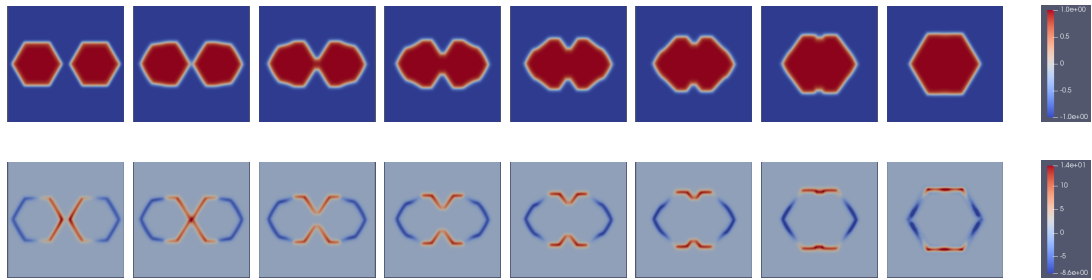
Figure 6: States (above) and corresponding controls (below) for the solution of splitting geometries.



(a) Result for 'merge circle' in the isotropic case.



(b) Result for 'merge square' with the regularized l_1 -norm.



(c) Result for 'merge hexagon' using the hexagon anisotropy.

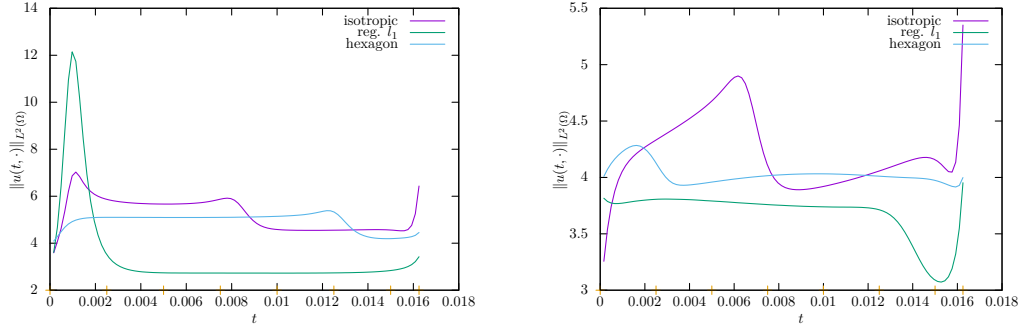
Figure 7: State (above) and corresponding control (below) for the solution of merge geometries.

	iso	l_1	hexa
$j(u)$	0.103955	0.0562286	0.0884921
$j_1 + j_2$	0.00409254 + 0.0998625	0.000728494 + 0.0555001	0.00115402 + 0.0873381

Table 5: Values of the cost functional for splitting geometries.

	iso	l_1	hexa
$j(u)$	0.0666414	0.0496374	0.0588482
$j_1 + j_2$	0.00274715 + 0.0638943	0.0010941 + 0.0485433	0.000905395 + 0.0579428

Table 6: Values of the cost functional for merging geometries.



(a) Results for ‘splitting’ cf. figs. 6a to 6c. (b) Results for ‘merging’ cf. figs. 7a to 7c.

Figure 8: Time evolution $\|u(t, \cdot)\|_{L^2(\Omega)}$ when topology changes are present.

Acknowledgements

The authors gratefully acknowledge the support by the RTG 2339 “Interfaces, Complex Structures, and Singular Limits” of the German Science Foundation (DFG).

References

- [1] M. Alfaro et al. “Motion by anisotropic mean curvature as sharp interface limit of an inhomogeneous and anisotropic Allen–Cahn equation”. *Proc. Roy. Soc. Edinburgh Sect. A* 140 (2010), pp. 673–706.
- [2] M. S. Alnæs et al. “The FEniCS Project Version 1.5”. *Archive of Numerical Software* 3 (2015).
- [3] J. W. Barrett, H. Garcke, and R. Nürnberg. “Numerical approximation of anisotropic geometric evolution equations in the plane”. *IMA J. Numer. Anal.* 28 (2007), pp. 292–330.
- [4] J. W. Barrett, H. Garcke, and R. Nürnberg. “A variational formulation of anisotropic geometric evolution equations in higher dimensions”. *Numer. Math.* 109 (2008), pp. 1–44.
- [5] J. W. Barrett, H. Garcke, and R. Nürnberg. “On the stable discretization of strongly anisotropic phase field models with applications to crystal growth”. *ZAMM Z. Angew. Math. Mech.* 93 (2013), pp. 719–732.
- [6] L. Blank and J. Meisinger. *Optimal control of a quasilinear parabolic equation and its time discretization*. 2021. arXiv: 2102.02616 [math.OC].
- [7] A. R. C. Clason V. H. Nhu. “Optimal control of a non-smooth quasilinear elliptic equation”. *Math. Control Relat. Fields* 11 (2021), pp. 521–554.

- [8] E. Casas and L. A. Fernández. “Boundary control of quasilinear elliptic equations”. Research Report RR-0782. INRIA, 1988.
- [9] E. Casas and L. A. Fernández. “Optimal control of quasilinear elliptic equations with non differentiable coefficients at the origin”. *Rev. Mat. Complut.* 4 (1991), pp. 227–250.
- [10] E. Casas and L. A. Fernández. “Distributed control of systems governed by a general class of quasilinear elliptic equations”. *J. Differential Equations* 104 (1993), pp. 20–47.
- [11] E. Casas and L. A. Fernández. “Dealing with integral state constraints in boundary control problems of quasilinear elliptic equations”. *SIAM J. Control Optim.* 33 (1995), pp. 568–589.
- [12] A. R. Conn, N. I. M. Gould, and P. L. Toint. *Trust Region Methods*. MPS-SIAM Series on Optimization. Society for Industrial and Applied Mathematics, 2000.
- [13] K. Deckelnick, G. Dziuk, and C. M. Elliott. “Computation of geometric partial differential equations and mean curvature flow”. *Acta Num.* 14 (2005), pp. 139–232.
- [14] J. J. Eggleston, G. B. McFadden, and P. W. Voorhees. “A phase-field model for highly anisotropic interfacial energy”. *Phys. D* 150 (2001), pp. 91–103.
- [15] C. M. Elliott and R. Schätzle. “The limit of the anisotropic double-obstacle Allen–Cahn equation”. *Proc. Roy. Soc. Edinburgh Sect. A* 126 (1996), pp. 1217–1234.
- [16] C. Gräser, R. Kornhuber, and U. Sack. “Time discretizations of anisotropic Allen–Cahn equations”. *IMA J. Numer. Anal.* 33 (2013), pp. 1226–1244.
- [17] M. Hinze et al. *Optimization with PDE Constraints*. Mathematical Modelling: Theory and Applications. Springer Netherlands, 2008.
- [18] R. Kobayashi. “Modeling and numerical simulations of dendritic crystal growth”. *Phys. D* 63 (1993), pp. 410–423.
- [19] A. Logg and G. N. Wells. “DOLFIN: Automated Finite Element Computing”. *ACM Trans. Math. Software* 37 (2010).
- [20] A. Miranville. “On an anisotropic Allen-Cahn system”. *Cubo (Temuco)* 17 (2015), pp. 73–88.
- [21] A. Rätz and A. Voigt. “Higher order regularization of anisotropic geometric evolution equations in three dimensions”. *J. Comput. Theor. Nanosci.* 3 (2006), pp. 560–564.
- [22] T. Steihaug. “The conjugate gradient method and trust regions in large scale optimization”. *SIAM J. Numer. Anal.* 20 (1983), pp. 626–637.
- [23] S. Torabi et al. “A new phase-field model for strongly anisotropic systems”. *Proc. Roy. Soc. Edinburgh Sect. A* 465 (2009), pp. 1337–1359.
- [24] G. Wachsmuth. “Differentiability of implicit functions: Beyond the implicit function theorem”. *J. Math. Anal. Appl.* 414 (2014), pp. 259–272.

- [25] G. Wachsmuth. “Optimal control of quasistatic plasticity with linear kinematic hardening, Part II: Regularization and differentiability”. *Z. Anal. Anwend.* 34 (2015), pp. 391–418.
- [26] G. Wachsmuth. “Optimal control of quasistatic plasticity with linear kinematic hardening, Part III: Optimality conditions”. *Z. Anal. Anwend.* 35 (2016).
- [27] S. M. Wise, J. Kim, and J. S. Lowengrub. “Solving the regularized, strongly anisotropic Cahn–Hilliard equation by an adaptive non-linear multigrid method”. *J. Comp. Phys.* 226 (2007), pp. 441–446.
- [28] M. Wolff and M. Böhm. “On parameter identification for general linear elliptic problems of second order”. Berichte aus der Technomathematik 18-01. Universität Bremen, Zentrum für Technomathematik, Fachbereich 3-Mathematik und Informatik, 2018.
- [29] G. Wulff. “XXV. Zur Frage der Geschwindigkeit des Wachstums und der Auflösung der Krystallflächen”. *Z. Kristallogr. – Cryst. Mater.* 34 (1901), pp. 449–530.
- [30] E. Zeidler and L. F. Boron. *Nonlinear Functional Analysis and its Applications: II/B: Nonlinear Monotone Operators*. Springer New York, 2013.